

***In situ* X-ray studies during extrusion of polyethylene**

J. W. H. Kolnaar* and A. Keller

H.H. Wills Physics Laboratory, Bristol University, Tyndall Avenue, Bristol BS8 1TL, UK

and S. Seifert, C. Zschunke and H. G. Zachmann

Institut für Technische und Makromolekulare Chemie, Bundesstrasse 45, 20146 Hamburg, Germany

Through the use of a high intensity synchrotron X-ray source and a specially constructed X-ray transparent flow cell, the feasibility of monitoring phase transformations *in situ* within the extruder has been demonstrated. Specifically, in the present experiments on polyethylene the emergence of a new, flow-induced phase was noted at around 150°C arising in the capillary portion of the rheometer consistent with the hexagonal crystal form of polyethylene. This 'mobile' mesophase would account for the recently discovered rheological melt flow singularity (the 'extrusion window') occurring at 150°C in agreement with previous hypotheses.

(Keywords: polyethylene; extrusion; X-ray diffraction)

Introduction

The general objective of the work reported in this communication is to monitor with X-rays what happens *within* an extruder in the course of polymer flow. The motivation for this work lies in extensive past material on phase transitions – solidification/crystallization effects in particular – of extrusion not too far above the stationary melting temperature^{1–10}. To our knowledge, the first publication of relevance with regard to the latter is that by van der Vegt and Smit¹. These authors performed standard rheological measurements using a capillary rheometer on polyolefins (polypropylene, polyethylene and ethylene propylene copolymers) and also natural rubber; however, in contrast to the usual practice, this was done not only at conventional processing temperatures (i.e. far above the melting point where the viscosity is lower) but also closer to temperatures where the respective materials solidify under stationary conditions in practice. They made the (at that time) unexpected observation that for sufficiently high strain rates (as calculated from plunger speed) the viscosity was rising (instead of falling, as for the usually expected shear thinning behaviour) with increasing rate, this rise proceeding to infinity, i.e. until complete cessation of flow, meaning blockage of the capillary at a critical flow rate. The solidified polymer blocking the flow in the form of a plug showed a very high degree of orientation by X-ray diffraction, corresponding to *c*-axis orientation in a usually drawn fibre.

van der Vegt and Smit interpreted the effect in question as the consequence of elongational flow-induced chain extension associated with the converging flow into the entry orifice; this raises the melting point, in turn leading to crystallization which, being from preoriented chains, leads to the macroscopic orientation observed.

The van der Vegt–Smit line of experimentation was pursued further in numerous studies by Porter and collaborators^{2,3} and by workers at Bristol University^{4–10}. The emphasis was on the product (plug) arising through the blockage, which showed advantageous properties – specifically high modulus (*c.* 70 GPa) and breaking strength (*c.* 3 GPa) – without the disadvantageous property of extensive fibrillation, placing the plug thus obtained in the ultrastiff and ultrastrong material category. The latter arises from the very high chain extension, making the C–C valence bonds along the practically fully stretched-out chain the stiffness and strength determining element.

Besides this general objective for *in situ* observations in the course of flow, a special effect has prompted the present investigations. This effect concerns a rheological melt flow singularity at a specific temperature during melt flow of high molecular weight polyethylene (PE) grades, which is the material of concern throughout this work. More specifically, it has been found^{11–18} that PEs, which owing to the interference of melt flow instabilities would be conventionally unextrudable, may become smoothly processable when the temperature is lowered to *c.* 148–152°C ('extrusion window'). Within this interval, smooth extrudability is accompanied by comparatively little die swell and a minimum in extrusion pressure (hence energy required to extrude the material). *Figure 1* shows a typical pressure (*p*) *versus* temperature (*T*) curve recorded using a slit-shaped capillary die and a conventional Davenport extruder described elsewhere¹⁷. Here the pressure minimum at 150°C should be strikingly apparent.

Contrary to the crystallization effects described above associated with pressure (viscosity) rise, which take place at temperatures below *c.* 148°C in *Figure 1* and rely on the entry orifice for their existence, this 'window' effect has been shown to originate within the simple shear flow field in the capillary of the extrusion die^{15–18}. Accordingly, the flow mechanism responsible

* To whom correspondence should be addressed
Present address: DSM Research, PO Box 18, 6160 MD Geleen, The Netherlands

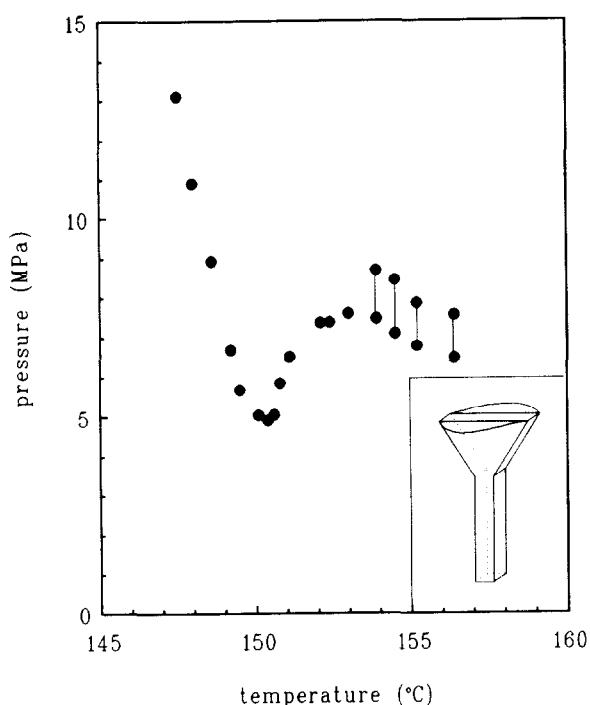


Figure 1 Steady-state pressure level as a function of temperature (T) using a planar die geometry (shown schematically in the inset). Capillary cross-section $2 \times 2 \text{ mm}^2$; capillary length 14 mm; angle of convergence 90° ; molecular weight 5.1×10^5 ($M_w/M_n \approx 4.9$); apparent wall shear rate $\dot{\gamma}_A \approx 2.0 \text{ s}^{-1}$. The vertical lines at $T > 154^\circ \text{C}$ denote pressure oscillations

for the singularity could be envisaged as slippage along the capillary wall.

Apart from having significant practical potential, the 'window effect' is also a major challenge scientifically. It cannot be explained in terms of melt rheology alone and, more specifically, the sharpness of the temperature of the pressure minimum^{11,15,17} and its invariance with extrusion rate^{11,15,17}, combined with the possibility that structure memory effects are at play^{12,15,17}, point to a thermodynamic origin, in particular a phase transformation. For this phase transition to occur, chain extension would be a precondition. Verification of the phase involved (the 'window' effect would require a mobile phase which could be the hexagonal phase of polyethylene) by *in situ* X-ray registration within the capillary, in this case originally arrived at from rheological inferences, would clearly be called for.

The requirements for experimentation are as follows.

- The use of high intensity X-rays, as the time-scale of measurement has to be short compared with the time-scale (i.e. rate) of flow.
- The technique should enable probing of material in preselected regions within the extruder. This has to be *in situ* under conditions where the rheological effect itself is being observed, preferably simultaneously, hence
- The rheometer must operate at just the right temperature and flow conditions.
- The optical part of the rheometer set-up should be capable of transmitting the X-rays.

These requirements necessitated construction of a

purpose-built rheometer including, among others, a flow cell with beryllium windows.

Experimental

Real-time wide angle X-ray diffraction (WAXD) experiments were conducted at HASYLAB, Deutsches Elektronen Synchrotron (DESY), Hamburg, Germany¹⁹. The radiation was monochromatized to a wavelength $\lambda \approx 0.154 \text{ nm}$ and collimated to a beam size of approximately $2 \times 1 \text{ mm}^2$ (vertical \times horizontal) using a series of slits. Data acquisition times could be reduced to typically 15 s. A one-dimensional detector equipped with 512 channels was used, which was positioned horizontally, hence only equatorial $\{hk0\}$ reflections could be observed. (For the present experiments a linear detector was used as maximum sensitivity was required. Knowing that in this way the effects in question can indeed be registered (see below), in future works a two-dimensional detector will also be employed.) The active length of the detector was approximately 80 mm and the sample-to-detector distance was approximately 115 mm. The recorded frames were corrected for air scatter and for the sensitivity of the detector. The sensitivity of the detector was determined employing the radiation of a ^{55}Fe source (average of 128 frames, each taken at a data acquisition time of 60 s). Corrections for the linearity of the detector (spatial corrections) were not applied.

In order to test for the transparency of the flow cell, a diffraction curve was first recorded of a PE sample crystallized from the melt within the rheometer at room temperature. The (corrected) WAXD-intensity data are depicted in Figure 2, showing the familiar pattern for solid PE consisting of two strong orthorhombic 110 and 200 reflections, thus demonstrating the transparency of the cell. The detector position (i.e. channel number) was calibrated against the double Bragg reflection angle (2θ) of these 110 and 200 reflections, as known from the literature²⁰: $2\theta = 21.73^\circ$ ($d = 0.409 \text{ nm}$), and $2\theta = 24.18^\circ$ ($d = 0.368 \text{ nm}$) respectively.

During the extrusion experiments, the force on the piston and the temperature close to the capillary were monitored continuously (the temperatures referred to in these experiments are estimated to be accurate within 1°C). The piston speed (i.e. geared motor speed) could be varied using a remotely placed control unit. The experimental set-up consisted of a 9.5 mm diameter cylindrical reservoir of 160 mm length and a slit-shaped die, a schematic drawing of which is given in Figure 3. The capillary length and width were 10 and 1.5 mm, respectively. The optical path length was 2.0 mm and the entrance angle to the capillary was 90° . The die was equipped with a set of 10 mm diameter beryllium windows, each of 2.0 mm thickness, and on exit of the X-ray beam a conical aperture of 60° was employed, hence all double Bragg reflection angles (2θ) up to *c.* 30° could be observed.

The material used in the *in situ* X-ray diffraction experiments was a linear PE with a weight-average molecular weight (M_w) of 2.8×10^5 ($M_w/M_n \approx 7.50$, HD6720pr200, supplier DSM). Samples were prepared for extrusion in the rheometer barrel by compaction of the fine grained powder at ambient temperature and melting at 180°C (30 min) to erase the nascent grain structure. After melting was completed, the barrel was cooled to preselected temperatures at which the polymer

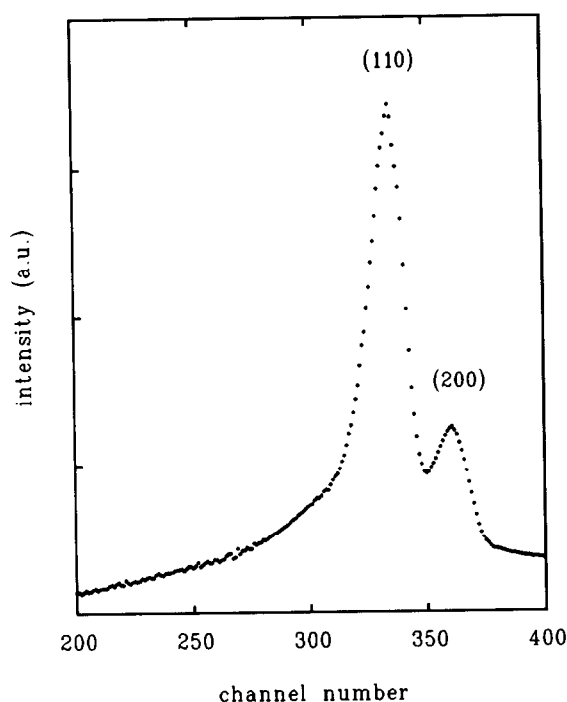


Figure 2 Intensity versus channel number on the linear detector (diffraction curve) for a solidified polyethylene sample at room temperature, showing the 110₀ and 200₀ reflections of the orthorhombic unit cell

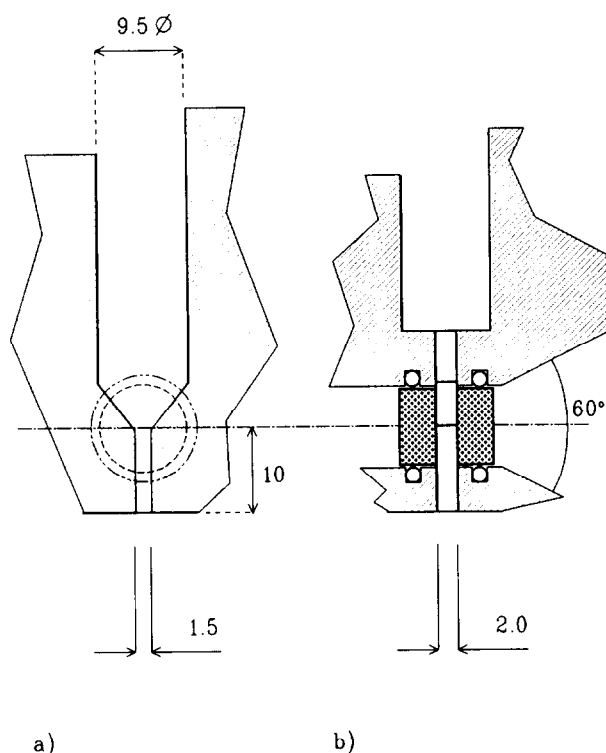


Figure 3 Sketch of the capillary die geometry used for *in situ* wide angle X-ray diffraction experiments. The direction of flow is from top to bottom. (a) Front view; the direction of the incident beam is perpendicular to the plane of drawing. (b) Side view; the direction of the incident beam is parallel to the plane of drawing (from left to right)

melt was conditioned for 15 min prior to starting the experiment. Gel permeation chromatography results had indicated previously that no significant degradation effects took place during this procedure.

Two temperature regions were investigated.

- (1) In order to demonstrate the feasibility of the *in situ* X-ray method adopted in the first set of experiments, the flow behaviour was investigated at temperatures in the region where flow-induced crystallization effects are present. For the polymer, die geometry and range of extrusion rates employed, these solidification effects were diagnosed in a region extending from 140 to 148°C. Since flow-induced crystallization effects are known to take place in the elongational flow field of the die, the X-ray beam was focused at the bottom part of the constriction, i.e. where the elongational flow rate is maximum (see Figure 3).
- (2) In the second set of experiments, the flow behaviour at temperatures corresponding to the 'temperature window' of the newly recognized effects (i.e. $T \approx 148\text{--}152^\circ\text{C}$) was investigated. Since these effects are assigned to processes occurring along the wall within the capillary of the die, the beam was focused on the centre of the capillary at a position as far downstream from the converging entrance zone as possible, while still providing sufficient scattering intensity (see Figure 3). (In these experiments the X-ray beam was focused perpendicular to the wall. Clearly, aligning the beam parallel to the wall would enable one to obtain more structural information. However, given the conical aperture of the diffraction cone on exit of the beam and taking into account the relatively large size of the X-ray beam (i.e. $2 \times 1 \text{ mm}^2$), only the central part of the flow field in the capillary could be made visible.) For the latter, a position c. 4 mm downstream in the capillary was found to be optimum.

Results and discussion

Experiments at temperatures close to the melting point.

In Figure 4 the (corrected) X-ray diffraction curves are given for the quiescent melt at an extrusion temperature of $T = 144^\circ\text{C}$ (bottom curve) and for the case of flow at decreasing temperatures of, respectively, 144, 143 and 142°C (from bottom to top; piston speed 3.5 mm min^{-1}). (From the piston velocity (v) the apparent wall shear rate ($\dot{\gamma}_A$) in the slit can be approximated as $\dot{\gamma}_A \approx 6Sv/D^2W$, where S = surface area of the cross-section, D = thickness and W = width of the slit.) The peak positions (channel numbers) of the 110 and 200 reflections in the top curve of Figure 4 ($T = 142^\circ\text{C}$) were recalibrated against the known double Bragg reflection angles of PE at high temperature, taken at $2\theta = 20.9^\circ$ and 22.2° , respectively²¹, see Table 1. (In view of the value of the corresponding Bragg reflection angles of the additional reflections in Figure 4, it was noticed that a considerable increase (c. 2°) relative to their room temperature calibration values ($2\theta = 21.73^\circ$ and 24.18°)²⁰ occurred during heating of the rheometer to 144°C . This shift towards higher 2θ values, hence lower d -spacings, is opposite to what is to be expected on the basis of thermal expansion, and is attributed to displacement of the flow cell relative to the detector during heating of the rheometer, thus causing an offset angle of the detector. During the single session available on the X-ray source this could not be checked, let alone rectified. The high temperature calibration will be maintained throughout

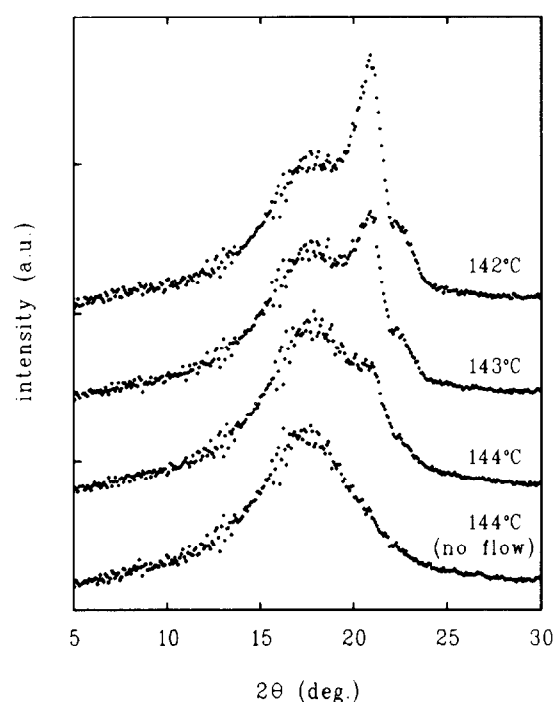


Figure 4 Intensity versus double Bragg reflection angle (2θ) as a function of temperature. Bottom curve: $T = 144^\circ\text{C}$ (no flow). Other curves: flow at $v = 3.5\text{ mm min}^{-1}$ ($\dot{\gamma}_A \approx 3.1\text{ s}^{-1}$). Extrusion temperatures increasing from top to bottom are indicated

Table 1 Peak positions of the 110_s , 200_s and 100_h reflections observed during melting of constrained or slightly crosslinked PE fibres ($\lambda = 0.154\text{ nm}$)

Temperature ($^\circ\text{C}$)	2θ 110_s (degree)	2θ 200_s (degree)	2θ 100_h (degree)	Ref.
25	21.73	24.18		20
100	21.3	23.0		21
145	20.9	22.2	20.2	21
149			20.5 ± 0.3	This work
150			20.3 ± 0.3	29
150	20.60	21.97	19.59	21
152			20.42	26

the rest of this work. The data from ref. 21 refer to related experiments, namely crosslinked ultradrawn polyethylene fibres capable of being heated close to the required temperature range without full melting of the crystals.) The peaks of the diffraction curve were curve-fitted using Pearson functions (i.e. convolution of Gaussian and Lorentz functions).

It is observed from Figure 4 that, through the action of flow, a pair of additional peaks appear beside the broad melt peak. Moreover, the intensities of both additional reflections are seen to rise sharply on lowering the temperature from 144 to 142°C . In accord with Figure 2 and by all previous experience¹⁻¹⁰ this additional pair of reflections may be attributed to the 110 and 200 reflections of the orthorhombic phase of PE.

It may be remarked even at this stage that this ready *in situ* identification of structures during extrusion is quite remarkable, if not totally unexpected. As well as confirming the formation of fibrous structures within a flowing melt at temperatures close to the solidification

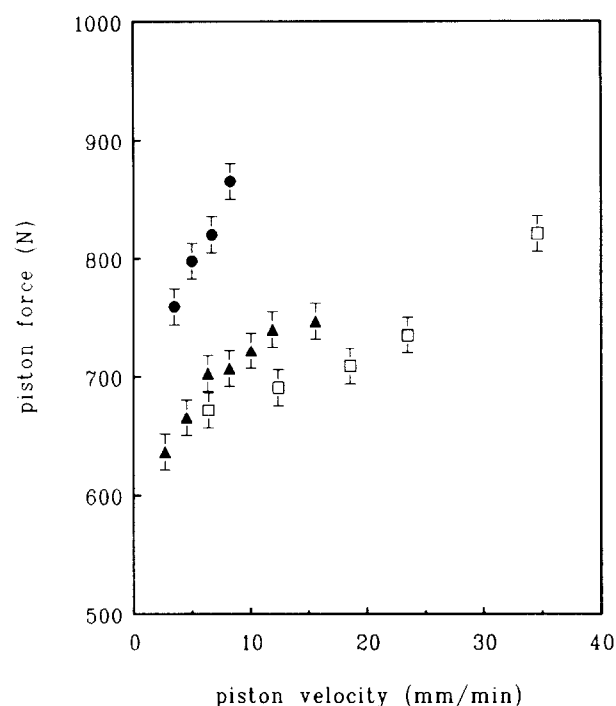


Figure 5 Piston force as a function of piston velocity for different temperatures of extrusion: (●) $T = 146^\circ\text{C}$, (□) $T = 149^\circ\text{C}$ (window) and (▲) $T = 152^\circ\text{C}$

point, it may also enable probing of flow-induced phase transformations in broader generality.

Experiments within the temperature 'window'. The piston force versus piston velocity trace recorded at 149°C (i.e. within the extrusion window) is shown in Figure 5, which also contains the curves obtained at 146°C and 152°C . At all temperatures in Figure 5, the forces exerted on the plunger increase with rising piston velocity, which is the expected behaviour. It is further observed that the piston forces, hence the corresponding pressure drops, at the temperature of 149°C are lower than those encountered at both the lower (146°C) and the higher (152°C) temperature of extrusion. Finally, the piston forces at 149°C are seen to rise less steeply with increasing piston velocity than is the case for the other extrusion temperatures. Both features are characteristic of the flow behaviour related to the temperature interval of the 'extrusion window' effect¹¹⁻¹⁸.

Having demonstrated the presence of the 'window' effect by means of rheological characterization in Figure 5, in Figure 6 the corresponding (corrected) X-ray diffraction curves are shown for the case of flow (top curve) and after cessation of flow (bottom curve) at $T = 149^\circ\text{C}$. (Note that for the sake of clear presentation in Figure 6 a constant has been added to the intensity for the case of flow in the top curve.) It is observed from Figure 6 that, for the piston velocity applied, a single shoulder appears at a value of spacing lower than that of the broad peak of the amorphous melt phase. (At the extrusion temperature of 150°C , qualitatively similar effects were observed. However, the intensity of the shoulder was even lower.)

At higher temperatures (152°C) the shoulder in Figure 6 vanishes (not shown), thus it may be concluded that the phase responsible for the small peak in Figure 6 must be

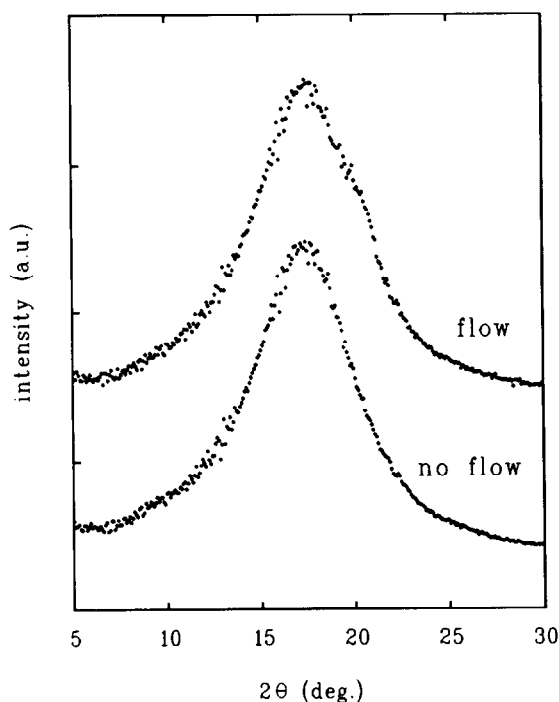


Figure 6 Intensity versus double Bragg reflection angle (2θ) curve at $T = 149^\circ\text{C}$ for the case without flow (bottom curve) and flow at $v = 35\text{ mm min}^{-1}$ (i.e. $\dot{\gamma}_A \approx 31\text{ s}^{-1}$) (top curve)

the origin of the anomalous flow behaviour at 149°C (displayed by Figure 5). It thus follows that the underlying cause for the occurrence of the 'extrusion window' is indeed in a phase transformation.

The next question to be addressed relates to the nature of this phase. In spite of difficulties in determining the peak position of the shoulder in Figure 6, a certain quantification could be made by curve-fitting, indicating that the double Bragg reflection angle of the unknown phase $2\theta_{hkl} \approx 20.5 \pm 0.3^\circ$. The peak position of the amorphous phase ($2\theta_{\text{melt}} \approx 17.5^\circ$) remains essentially unaltered upon increasing the temperature from 146 to 149°C (compare Figures 4 and 6).

It has been hypothesized in previous works^{11–18} that the rheological effect requires a phase that is 'slippery', hence one possessing high mobility. Such a mobile phase could be the hexagonal phase. At ambient and/or stationary conditions this hexagonal phase is known to be metastable. However, several experimental conditions may be created where the hexagonal phase in polyethylene may become the stable one, such as by applying high pressure^{22–24}, by application of external constraints during melting of a highly oriented polyethylene fibre^{25–27} or during melting of irradiated PE fibres^{21,28–30}.

With regards to the relative value of the d -spacings, Table 1 should serve as an illustration showing the peak positions of the orthorhombic (subscript o) and hexagonal (subscript h) phase from constrained melting experiments on ultra-oriented ultra-high molecular weight PE fibres^{25–27} and slightly crosslinked PE fibres^{21,28–30}.

Table 1 indicates that the difference in peak position between the 110_o reflection and the 100_h reflection at temperatures around 150°C and at ambient pressure is around 0.7 – 1° . In the present case the difference in 2θ

between the newly formed phase at 149°C and the 110_o reflection at 142°C amounts to $c. 0.4^\circ$ (i.e. $2\theta_{110} = 20.9^\circ$ at 142°C and $2\theta_{hkl} = 20.5^\circ$ at 149°C). Taking into account the accuracy limits of the determination of the position of the shoulder in Figure 6 ($\pm 0.3^\circ$), it follows that the new phase could well be the hexagonal one.

In principle, the verification of a crystalline unit cell would require the availability of several crystalline reflections. Even so, within certain limits an attribution is possible on the basis of evidence available. In Figure 6 only one reflection is apparent. In the case of the usual orthorhombic phase at least the two most intense reflections (i.e. the 110 and the weaker 200) would be expected to be visible, as is indeed the case in Figure 4. It is seen that the weaker 200 is still distinct in the 144°C trace (with flow), in contrast to the similar but somewhat weaker reflection (from the point of view of the amount of crystallinity) in Figure 6. Clearly an equally intense trace, with regard to the crystal reflection, would be required to make this comparison conclusive in itself. At this stage it can at least be stated that, within the present limitation, there is no evidence for a second reflection such as that required by the orthorhombic phase. (Another possibility relates to the monoclinic phase, which has sometimes also been referred to as triclinic. It is known that during deformation the orthorhombic phase may sometimes transform into the monoclinic phase³¹ – for reviews see refs 32 and 33. This martensitic transition has, however, never been observed at temperatures as high as 150°C . Moreover, on the basis of the above argument, the presence of a monoclinic phase would also have required more than a single reflection.) This is in line with the expectation, from all previous experience, that the formation of fibrous orthorhombic crystals proper would block and not promote flow, which is the present observation.

The next question relates to the spacing value of the registered reflection. As apparent, the spacing of the shoulder is somewhat larger (and the diffraction angle is smaller) than that of the 110 reflection of the orthorhombic phase and is within the range normally assigned to the 100 reflection of the hexagonal phase, even if on the small side of this range. This, together with the fact that within the limits of our registration sensitivity there is only a single reflection, coupled with the plausible argument that the newly formed phase is promoting and not blocking the flow, is strongly in favour of its assignment to the hexagonal phase. Accordingly, in addition to its manifold previous manifestations (see refs 34–36), this mesomorphic state of PE would now seem to appear under new circumstances (i.e. in capillary flow, presumably along the walls) giving rise to the 'window' effect, as surmised previously on the strength of the entire rheological experience.

A further comment which needs to be made concerns the amount of the newly formed phase responsible for the 'window' effect. Figure 6 shows that the intensity of the peak associated with this phase is very low in comparison with that of the amorphous phase. From all previous evidence^{15–18} the relevant changes are most likely to be confined to the walls of the conduit. It is inferred above that, despite the limits imposed by the finite size of the X-ray beam and the conical aperture of the exit beam on the portion of the flow field available for examination, the amount of material being transformed

into the new phase can only be minute (i.e. of the order of 1%). This would imply that the presence of only a very small amount of this phase could have considerable effects on the flow in the capillary. This should be compared with general extrusion practice where (external) lubricants, such as fluoropolymers, are added to decrease the interaction between a solid wall and the flowing polymer and hence to make the melt flow more readily. More specifically, it is known that addition of merely a fraction of a per cent of lubricant can give rise to substantial reductions of extrusion pressures. In fact, it has been demonstrated that the flow behaviour in the 'extrusion window' has many similarities to such lubricated flows¹⁵.

Finally, although the attribution of the flow singularity to the capillary portion of the die seems unquestionable on the basis of extensive rheological evidence, the relation, if any, between the physical effects arising in the capillary and those at the entry orifice remains an open question. This will be commented on in a forthcoming paper³⁷.

Conclusions

In situ X-ray experiments using the synchrotron source at DESY have established the feasibility of monitoring phase transformations in the course of flow during extrusion. They have further provided evidence for the creation of a hexagonal phase in polyethylene under conditions which have not been reported previously in the literature. As such, the recognition of the hexagonal phase should provide an explanation for a recently discovered melt flow singularity ('extrusion window') occurring during flow of polyethylene at around 150°C.

Acknowledgements

Financial support by DSM, The Netherlands, is gratefully acknowledged by one of us (J.W.H.K.). We wish to thank Gerrit Martens (DSM) for assisting in the design and manufacture of the rheometer equipment. We are grateful to Dr Phil Barker and Dr Hartmut Fischer for assisting in the processing of the X-ray data.

References

- 1 van der Vegt, A. K. and Smit, P. P. A. *Adv. Polym. Sci. Technol.* 1967, **26**, 313
- 2 Porter, R. S. and Johnson, J. F. *Trans. Soc. Rheol.* 1967, **11**, 259
- 3 Southern, J. F. and Porter, R. S. *J. Appl. Polym. Sci.* 1970, **14**, 2305
- 4 Farrell, C. J. and Keller, A. *J. Mater. Sci.* 1977, **12**, 966
- 5 Keller, A. and Odell, J. A. *J. Polym. Sci., Polym. Symp.* 1978, **63**, 155
- 6 Odell, J. A., Grubb, D. T. and Keller, A. *Polymer* 1978, **19**, 617
- 7 Bashir, Z., Odell, J. A. and Keller, A. *J. Mater. Sci.* 1984, **19**, 3713
- 8 Bashir, Z., Odell, J. A. and Keller, A. *J. Mater. Sci.* 1984, **21**, 3993
- 9 Bashir, Z. and Keller, A. *Colloid Polym. Sci.* 1989, **267**, 116
- 10 Bashir, Z. and Odell, J. A. *J. Mater. Sci.* 1993, **28**, 1081
- 11 Waddon, A. J. and Keller, A. *J. Polym. Sci.* 1990, **28**, 1063
- 12 Narh, K. A. and Keller, A. *Polymer* 1991, **32**, 2512
- 13 Narh, K. A. and Keller, A. *J. Mater. Sci. Lett.* 1991, **10**, 1301
- 14 Waddon, A. J. and Keller, A. *J. Polym. Sci. (B) Polym. Phys.* 1992, **30**, 923
- 15 Kolnaar, J. W. H. PhD Thesis, University of Bristol, 1993
- 16 Keller, A. and Kolnaar, J. W. H. *Prog. Colloid Polym. Sci.* 1993, **92**, 83
- 17 Kolnaar, J. W. H. and Keller, A. *Polymer* 1994, **35**, 3863
- 18 Kolnaar, J. W. H. and Keller, A. *Polymer* 1995, **36**, 821
- 19 Elsner, G., Riekel, Ch. and Zachmann, H. G. *Adv. Polym. Sci.* 1984, **67**, 3
- 20 Walter, N. M. and Reding, J. J. *J. Polym. Sci.* 1956, **21**, 561
- 21 Hikmet, R. M. PhD Thesis, University of Bristol, 1987
- 22 Bassett, D. C., Block, S. and Piermarini, G. J. *J. Appl. Phys.* 1974, **45**, 4146
- 23 Bassett, D. C. and Turner, B. *Phil. Mag.* 1974, **29**, 925
- 24 Yasuniwa, M., Enoshita, R. and Takemura, T. *Jpn J. Appl. Phys.* 1976, **19**, 4121
- 25 Pennings, A. J. and Zwiijnenburg, A. *J. Polym. Sci., Polym. Phys. Edn* 1979, **17**, 1011
- 26 van Aerle, N. A. J. M., Lemstra, P. J. and Braam, A. W. M. *Polym. Commun.* 1989, **30**, 7
- 27 Rastogi, S. and Odell, J. A. *Polymer* 1993, **34**, 1523
- 28 Clough, S. B. *Polym. Lett.* 1970, **8**, 519
- 29 Clough, S. B. *J. Macromol. Sci.* 1970, **B4**, 199
- 30 Hikmet, R. M., Lemstra, P. J. and Keller, A. *Colloid Polym. Sci.* 1987, **265**, 185
- 31 Frank, F. C., Keller, A. and O'Connor, A. *Phil. Mag.* 1958, **3**, 64
- 32 Bevis, M. and Crellin, E. B. *Polymer* 1971, **12**, 666
- 33 Young, R. J. and Bowden, P. B. *Phil. Mag.* 1974, **29**, 1061
- 34 Ungar, G. and Keller, A. *Polymer* 1980, **21**, 1273
- 35 Keller, A. and Ungar, G. *J. Appl. Polym. Sci.* 1991, **42**, 1683
- 36 Ungar, G. *Macromolecules* 1986, **19**, 1317
- 37 van Bilsen, H. M. M., Fisher, H., Kolnaar, J. W. H. and Keller, A. *Macromolecules* (submitted)